JCTC Journal of Chemical Theory and Computation

Article

pubs.acs.org/JCTC

NO_x Catalyzed Pathway of Stratospheric Ozone Depletion: A Coupled Cluster Investigation

Achintya Kumar Dutta, Nayana Vaval, and Sourav Pal*

Physical Chemistry Division, National Chemical Laboratory (CSIR), Pune-411008, India

Supporting Information

ABSTRACT: We report a theoretical investigation on the NO_x catalyzed pathways of stratospheric ozone depletion using highly accurate coupled cluster methods. These catalytic reactions represent a great challenge to state-of-the-art *ab initio* methods, while their mechanisms remain unclear to both experimentalists and theoreticians. In this work, we have used the so-called "gold standard of quantum chemistry," the CCSD(T) method, to identify the saddle points on NO_x-based reaction pathways of ozone hole formation. Energies of the saddle points are calculated using the multireference variants of coupled cluster methods. The calculated activation energies and rate constants show good agreement with available experimental results. Tropospheric precursors to stratospheric NO_x radicals have been identified, and their potential importance in stratospheric chemistry has been discussed. Our calculations resolve previous conflicts between *ab initio* and experimental results for a trans nitro peroxide intermediate, in the NO_x catalyzed pathway of ozone depletion.

I. INTRODUCTION

The stratospheric ozone layer constitutes an important part of earth's atmosphere. It absorbs light of wavelengths below 240 nm and saves the planet earth and life on it from lethal solar ultraviolet (UV) radiation. The past 50 years have seen a remarkable decrease in the concentration of the ozone layer. Thus, understanding the pathways of ozone depletion and its chemistry is of great importance for the prevention of it's decrease (Figure 1).

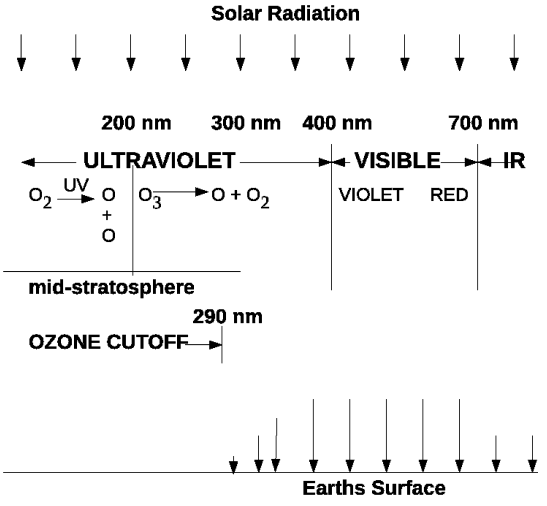

Figure 1. Atmospheric window for solar radiation.

It is well established that the "ozone hole" forms over the Antarctic due to reactions of ClO with ozone in the Antarctic spring.[1−4] This occurs because the vortex is strong over the Antarctic (due to fewer land masses relative to the northern hemisphere) and thus long-lived, and also because all of the nitrogen compounds are frozen out on polar stratospheric clouds (PSC) in the winter, and these "fall" out of the stratosphere into the troposphere, thereby depleting the air in the vortex of nitrogen. This is important, because the main reservoir compound for Cl is $ClONO_2$. Hence, in the spring time, the existing Cl compounds in the Antarctic vortex (ClOOCl, ClOOH, HOCl, etc.) are photolyzed and begin to react catalytically to destroy ozone, which continues to occur until the vortex breaks up.

The possibility of stratospheric ozone depletion via the NO_x catalyzed pathway was first postulated by Johnston[5] and supported by several model calculations.[6−9]

$$NO + O_3 \rightarrow NO_2 + O_2 \quad (1)$$

$$NO_2 + O \rightarrow NO + O_2 \quad (2)$$

Knowledge of the mechanism and kinetic parameters of reactions 1 and 2 is therefore of crucial importance in order to calculate ozone profiles in the stratosphere and to make reliable models of atmospheric ozone phenomena. Not surprisingly, the NO_x catalyzed reactions became much studied experimentally over the years so as to determine the associated rate constants and unravel the mechanistic details.[10−14] In spite of the relative abundance of experimental work, theoretical studies of NO_x based reactions of ozone depletion are rather scarce in the literature. The reported theoretical works are mostly done at the DFT and MP2 levels,[15,16] which is inadequate to account for the correlation effects in a systematic manner. Some of the papers report single point calculations at the CCSD[17] level, which takes care of the dynamic correlation in a satisfactory way. However, T1 diagonosis[18] indicates large multireference character of the species involved. Thus, it becomes necessary to handle nondynamic correlation in a proper way, which single reference coupled cluster fails to do. A multireference coupled

Received: January 2, 2012

dx.doi.org/10.1021/ct300209s | J. Chem. Theory Comput. XXXX, XXX, XXX−XXX

cluster (MRCC)[24,25] method can account for both dynamic and nondynamic correlation in a systematic way. But, so far, no multireference coupled cluster study has been done on NO_x catalyzed reactions. The objective of the present study is to carry out *ab initio* calculations of a sufficiently high level and to get accurate results for the study of the reaction of NO_x molecules with ozone in the context of stratospheric ozone depletion. We have used Fock space multireference (FSMRCC) theory for our study. FSMRCC is an effective Hamiltonian based theory and is known to give accurate direct difference energies.[19−21] It treats both N and $N \pm 1$ states on an equal footing. This method has been used extensively for difference energies and response properties of open-shell molecules and molecular excited states.[27]

This paper is organized as follows. The next section presents computational details. Results and discussion are followed in section III. The last section presents the conclusions and a brief discussion about the scope of future work.

II. METHODOLOGY AND COMPUTATIONAL DETAILS

We have optimized all of the structures using the ROHF-CCSD(T) method. There exist several variants of ROHF-CCSD(T). Specifically, we have used the variant developed by Bartlett and co-workers.[26] The aug-cc-pVTZ basis set[33] has been used for geometry optimization. For all subsequent calculations presented in the paper, the same basis set has been used. Following the geometry optimization, the frequency calculations have been done to determine the nature of the saddle point. Table 1 presents results of IR spectra and

Table 1. Comparison of Theoretical Calculated Frequency in the aug-cc-pVTZ Basis Set with Experimental Values for Ozone and Nitric Oxide

Ozone					
method	r_e (Å)	θ (deg)	ω_1 (cm^{-1})	ω_2 (cm^{-1})	ω_3 (cm^{-1})
DFT (B3LYP)	1.255	118.2	745	1188	1248
MP2	1.283	116.6	741	1157	2244
CCSD(T)	1.269	117.1	720	1062	1160
EXP	1.272[a]	116.82[a]	716[b]	1089[b]	1135[b]

Nitric Oxide		
method	r_e (Å)	ω (cm^{-1})
DFT (B3LYP)	1.145	1967
MP2	1.137	3336
CCSD(T)	1.151	1925
EXP	1.151[a]	1876[b]

[a]:see ref 36a [b]:see ref 36b

equilibrium geometry using different methods. It is clear from the table that only CCSD(T) results can give experimental accuracy. So, it is justified to use the CCSD(T) level of methods for the investigation of reactions involving NO_x and ozone, rather than MP2 and DFT.

Further, Table 2 presents the T1 diagnosis[18] values of reactants, products, and saddle points. It shows values higher than the permissible range of 0.02 (see Table 2), indicating the multireference nature of the wave function. To include the multireference effects, the FSMRCC method has been used to carry out the single point energy calculations on the optimized saddle points. FSMRCC is a valence-universal variant of multireference coupled cluster theory, and it is size-extensive

Table 2. T1 Diagnosis Values of the Involved Species

species	T1 value
O_3	0.029
NO_2	0.026
NO	0.040
N_2O	0.028
N_2O_2TS1	0.022
N_2O_2min	0.021
N_2O_2TS2	0.022
ONOOO	0.039
ONOO	0.035

for both ground and excited states. Photodissociation energies are calculated using the Equation Of Motion Coupled Cluster (EOMCC)[28] method. EOMCC is similar to FSMRCC and was successfully used by Bartlett and co-workers for the simulation of UV/vis absorption spectra for atmospheric modeling.[29]

All of the rate constants presented in the paper have been estimated from theoretically calculated barrier heights, using the Arrhenius equation. Pre-exponential factors are obtained from experimental data[43]

All of the ROHF-CCSD(T) calculations on NO_x catalyzed reactions have been performed using CFOUR.[30] Gaussian 09[31] has been used for some exploratory MP2, DFT-B3LYP, T1 diagnosis, and EOMCC calculations. FSMRCC single point calculations have been done using codes developed by Pal and co-workers.[32]

III. RESULTS AND DISCUSSION

First, it is necessary to find out among all of the NO_x radicals generated in the troposphere, which are probable candidates for stratospheric ozone depletion.

A. Tropospheric Precursors. To become a potential threat to the stratospheric ozone layer, NO_x radicals produced in the troposphere must satisfy certain conditions. First, it must be transparent to radiation of $\lambda > 290$ nm, so that it does not get destroyed by visible solar radiation in the troposphere. Moreover, the radicals must be sufficiently inert to reach the stratosphere in intact condition.

Excitation of NO_x radicals to higher electronic states by visible (400−700 nm) and UV (10−400 nm) light actually causes photodissociation. We have used the EOMCC method on previously reported potential energy surfaces[39] to calculate the corresponding excitation energies. Calculated wavelengths for all three species correspond to the highest absorption cross-section in experimental UV−visible absorption spectra of the species.[34] So light of this particular wavelength's can be taken as the major responsible radiation for the photo dissociation of the species. Table 3 represents photodissociation wavelengths and oscillator strengths of the precursor species. From Table 3, it can be seen that NO_2 will be destroyed within the troposphere

Table 3. EOMCCSD Calculated Photodissociation Energy of the NO_x Radicals

radical	excited state	photodiss. energy (nm)	oscillator strength	exptl. photodiss. energy (nm)[a]
NO_2	$^2B_2$	376	0.0099	372−402[b]
NO	$^2B_2$	198	0.0014	190−202[c]
N_2O	$^2A_1$	176	0.0000	176−187[b]

[a]In units of $10^{20}\sigma$ (cm^2). [b]See ref 34. [c]See ref 35.

dx.doi.org/10.1021/ct300209s | J. Chem. Theory Comput. XXXX, XXX, XXX−XXX

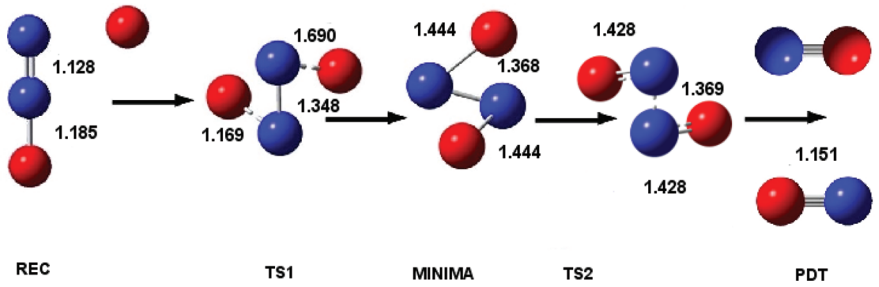

Figure 2. Formation of NO from N_2O.

by visible solar radiation. Now, both NO and N_2O are transparent to visible light. But, nitric oxide, being an odd-electron molecule, is highly reactive toward hydroperoxide and organic radicals.[40,41] Thus, finally, a negligible amount of nitric oxide enters the stratosphere. Our calculated values of photodissociation energy are in good agreement with the experimental values.

$$NO + HO_2 \rightarrow NO_2 + OH \quad (3)$$

$$NO + RO_2 \rightarrow NO_2 + RO \quad (4)$$

Now, N_2O does not have a significant sink in the troposphere. Therefore, nitrous oxide is the major source of odd nitrogen (NO_x) in the stratosphere and plays a fundamental role in regulating the ozone layer.[9,42]

B. Generation of NO. Nitric oxide is the main active species in the NO_x catalytic cycle of stratospheric ozone depletion. Tropospheric N_2O, after reaching the stratosphere, reacts with the present odd oxygen atom (^1D) to form NO. This nitric oxide enters into the catalytic ozone depletion cycle.

$$N_2O + O \rightarrow NO + NO \quad (5)$$

The first step of the reaction is the formation of a saddle point of order 1 (TS1). It has C_S symmetry and has an imaginary frequency of 431 cm^{-1} at the ROHF-CCSD(T) level of theory. The imaginary frequency corresponds to the vibration of normal modes along the reaction coordinate. The evolution of the saddle point is thus toward an ONNO intermediate with C_2 symmetry. This point has been characterized as a minimum (MINIMA), and it is the intermediate compound in the reaction, responsible for the generation of nitric oxide in the stratosphere.

From the MINIMA, nitric oxides are finally reached through a second transition state (TS2). This saddle point shows an imaginary frequency of 157 cm^{-1}. It shows very small perturbations of the geometrical parameter, compared to those of MINIMA, as expected from their small energy difference. Figure 2 shows the evolution from MINIMA to TS2 and from TS2 to products accompanies gradual shortening of the terminal N−O bonds and the consequent stretching of the N−N bond.

We have plotted the energies of the reactants, products, and saddle points, calculated using the FSMRCC method, in an energy profile diagram (Figure 3). It shows a barrier-less formation of the first transition state (TS1). It is 4.6 kcal/mol more stable than the reactants. There exists a minimum which is of 6.9 kcal/mol more stable than the TS1. The evolution from MINIMA to TS2 is the rate determining step in the reaction. The step shows a very low barrier height of 0.18 kcal/mol. This is expected from the very small perturbation of the geometrical parameter of TS2, compared to that of MINIMA.

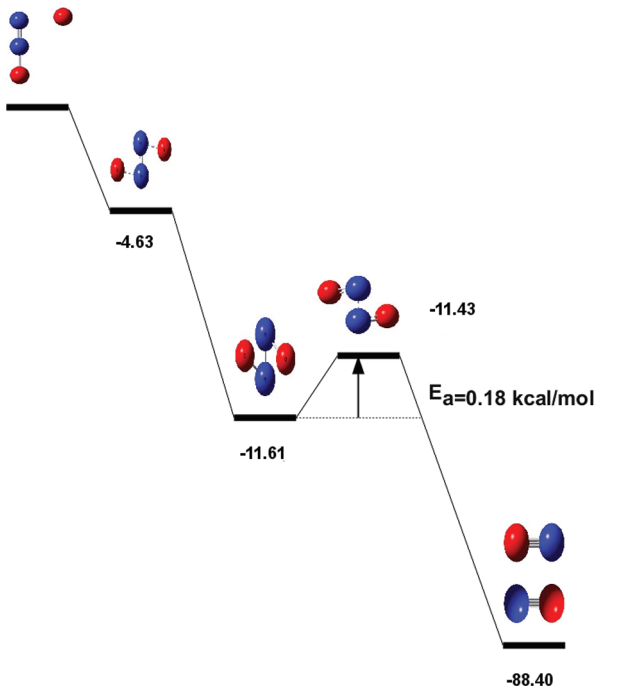

Figure 3. Energy profile diagram of the reaction between N_2O and O.

Table 4 shows that the calculated rate constant for the reaction is 4.9×10^{-11} cm^3 $molecule^{-1}$ S^{-1} at 298 K, which is very close to the experimental value of 6.7×10^{-11} cm^3 $molecule^{-1}$ S^{-1}).[43] The value of the used prefactor is 6.7×10^{-11} cm^3 $molecule^{-1}$ S^{-1}.

Table 4. Kinetic Parameter of the Reaction between N_2O and O

parameter	calculated	experimental[43]
E_a (kcal/mol)	0.18	
k (cm^3 $molecule^{-1}$ S^{-1}) at 298 K	4.9×10^{-11}	6.7×10^{-11}

All of the saddle points considered above are of trans configuration. There may be a possibility of a cis pathway. But all cis conformers have been found to be of equal energy to the corresponding trans isomer.

C. Beginning of the Catalytic Cycle. The nitric oxide generated from N_2O comes in contact with stratospheric ozone. According to the previous theoretical work of Dupuis et. al[44] for the H + O_3 reaction, the approach of the NO radical to the ozone molecule is determined by π orbitals of the terminal oxygen atom of ozone, as depicted in Figure 4. The first step of the reaction mechanism is the formation of a trans TS of C_1 symmetry. The imaginary frequency corresponding to the

dx.doi.org/10.1021/ct300209s | J. Chem. Theory Comput. XXXX, XXX, XXX−XXX

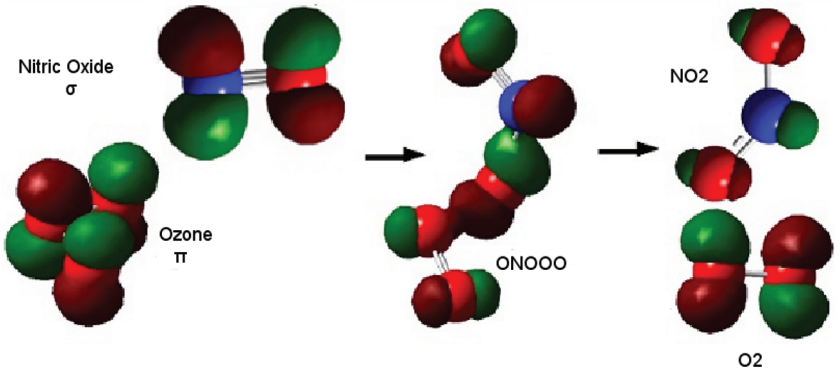

Figure 4. MO diagram representation of the reaction between O_3 and NO.

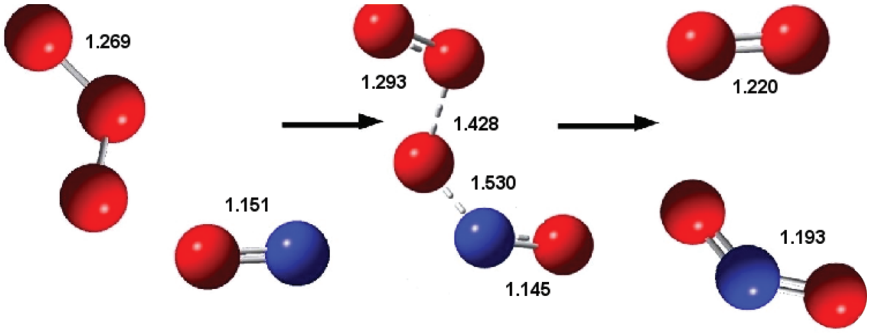

Figure 5. Trans pathway of the reaction between ozone and NO.

reaction coordinates is 292 cm^{-1}. Figure 5 shows that the formation of the TS involves stretching of one O−O bond of ozone, with subsequent formation of an O−N bond with nitric oxide. The TS then breaks down to nitric oxide and molecular oxygen. Table 5 reports the calculated value of activation energy and rate constants at the FSMRCC level of theory for the trans ONOOO transition state along with the experimental values. The activation energy for the reaction, calculated at the FSMRCC level, is 3.14 kcal/mol. With ZPE correction, the value comes down to 3.11 kcal/mol, which is well within the range of experimentally determined values between 1.44 and 3.18 kcal/mol (Figure 6).[45] Taking the standard prefactor (A) of 2×10^{-12}, the rate constant becomes 1.0×10^{-14} cm^3 $molecule^{-1}$ S^{-1}, at 298 K, which shows excellent agreement with the experimental value[43] of 1.8×10^{-14} cm^3 $molecule^{-1}$ S^{-1} (Table 5), which can be attributed to the high level of the method and the proper basis set being employed for the estimation of the barrier heights. However, there can always be a possibility of a fortuitous error cancellation leading to a better agreement.

Table 5. Kinetic Parameter of the Reaction between NO and O_3 at 298 K

parameter	calculated	experimental
E_a (kcal/mol)	3.11	1.4−3.18
k (cm^3 $molecule^{-1}$ S^{-1})	1.0×10^{-14}	1.8×10^{-14}

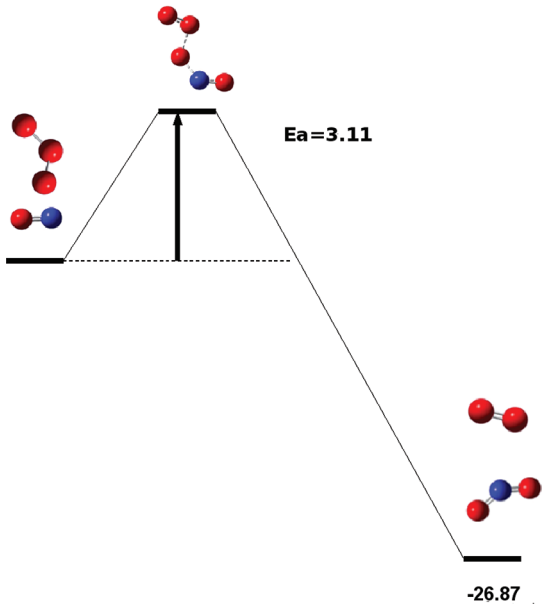

Figure 6. Energy profile diagram of reaction between ozone and NO.

D. Regeneration of Nitric Oxide. The nitrogen dioxide molecule, thus formed, reacts with odd oxygen (O) to regenerate NO (Figure 7). The reaction involves the formation of a trans nitro-peroxide radical intermediate, which then undergoes photodissociation to form two molecules of nitric oxide. Table 6 reports the EOMCC calculated photodissociation energy and the corresponding experimental values. It can be seen that the wavelength of photodissociation is 586 nm. This is well within the experimental range of 587 ± 4.[46] The NO radical, thus regenerated, again reacts with another ozone molecule, and the catalytic depletion cycle continues.

However, there are controversies about the existence of the doublet trans peroxo nitrate intermediate in reality.[47,48] The only reliable experimental data come from an IR frequency study of a probable trans ONOO intermediate, by Hall and Bhatia.[14] Their conclusion was based on the 50 cm^{-1} isotopic

dx.doi.org/10.1021/ct300209s | J. Chem. Theory Comput. XXXX, XXX, XXX−XXX

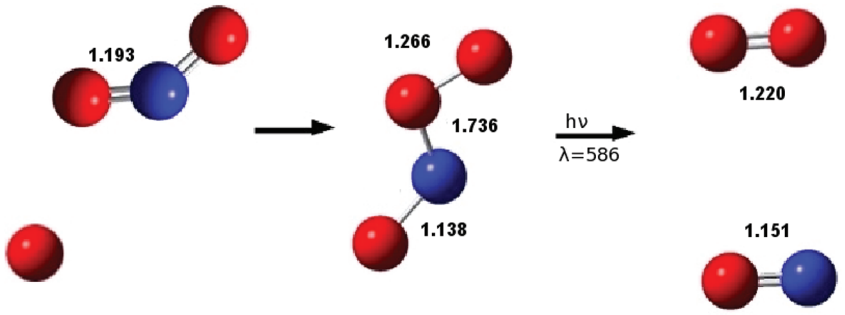

Figure 7. Regeneration of nitric oxide from NO_2.

Table 6. EOMCCSD Calculated Photodissociation Energy of the trans ONOO Radicals

basis set	photodissociation energy (nm)	experimental (nm)[46]
aug-cc-pVTZ	586	587 ± 4

shift of an IR band at 1840 cm^{-1}. They have tried to further support their hypothesis using some limited *ab initio* calculations[49] of structures and vibrational frequencies. However, their theoretically calculated results clearly deviate from experimental values. When we revisited the problem with the highly correlated CCSD(T) method and the aug-cc-pVTZ basis set, we obtained a good agreement with experimental results. Table 7 reports the values of IR frequency, intensity,

Table 7. Trans ONOO aug-cc-pVTZ IR Spectroscopy Results

frequencies (ω), cm^{-1}	I^{IR}, km·mol^{-1}	ω,[a] cm^{-1}	I^{IR},[a] km·mol^{-1}	exptl. freq., cm^{-1}	calcd. iso shift, km·mol^{-1}	exptl., cm^{-1}
123	1	207	1		−3	
198	1	469	1		−5	
271	3	671	13		−8	
719	3	976	100		−16	
1223	133	1287	14		−33	
1880	408	1659	7	1840	−49	−50

[a]Values calculated by Hall et al. *J. Phys. Chem.* **1994**, *90*, 7414 at the UHF level with the 6-31G* basis set.

and isotropic shift calculated at the ROHF-CCSD(T) level of theory in the aug-cc-pVTZ basis set, along with the experimental results. Table 7 also presents the value of IR frequency and intensity calculated at the UHF level with a 6-31G* basis set. A close inspection of Table 7 shows that, with the UHF method, the IR peak nearest to the experimental value deviates by 181 wavenumber. Moreover, the mode is of very low intensity (6.5 km·mol^{-1}). The only intense peak (100 km·mol^{-1}) in the spectrum is at 975.5 cm^{-1}, which is nearly half of the experimental frequency. So these theoretical results are not at all consistent with experiments. The reason is the inadequacy of the theoretical method and small basis set.

In the ROHF-CCSD(T) method with the aug-cc-pVTZ basis set, the highest peak is at 1880 cm^{-1}, very close to the experimental value of 1840 cm^{-1}. Moreover this peak is of very high intensity (408 km·mol^{-1}). This result is consistent with the experimental report of only one peak at 1840 cm^{-1}. Moreover, CCSD(T) calculation of the isotropic shift gives a value of −49 cm^{-1} for the highest peak, which is nearly identical to an experimental shift of −50 cm^{-1}. Thus, from the previous experimental data and our calculated results, it would be safe to conclude that a trans peroxo nitrate intermediate does get formed in the reaction between NO_2 and atomic oxygen.

E. Conclusions. In this paper, the NO_x catalyzed pathway of stratospheric ozone depletion has been computationally investigated with the coupled cluster method. The optimizations are performed at the ROHF-CCSD(T) level of theory in aug-cc-pVTZ basis set, while energetics of the reactions are investigated with the FSMRCC method in the same basis set.

Our EOMCC calculations show that among several probable tropospheric precursor compounds, only nitrous oxide is photochemically inert enough to move through the troposphere to reach the stratosphere. In the stratosphere, it reacts with an odd oxygen atom (^1D) to form the active catalytic species nitric oxide. The reaction evolves through the formation of a four-membered reaction intermediate. Our calculations suggest that the breaking of the N−N bond of the intermediate is the rate-determining step of the reaction, which is consistent with the experimental value of the rate constant for the reaction.

The first step of the NO_x catalytic cycle is the reaction of NO with an ozone molecule to form NO_2 and O_2. The reaction proceeds through a five-membered transition state of trans configuration and shows a barrier height of 3.11 kcal/mol. This agrees perfectly with the experimental range of activation energy.

The regeneration of nitric oxide from NO_2 involves the formation of a trans peroxo nitrate intermediate. Our calculation resolves the previous conflict between theoretical calculations and experimental results. It has been shown that the compound gives an intense IR peak at 1880 cm^{-1}, which is consistent with the experimental results. Thus, theoretical calculations can not only predict but also supplement experimental findings.

Hence, high level theoretical studies can give a better understanding of the NO_x based pathways of stratospheric ozone depletion for both theoreticians and experimentalists. It would be interesting to extend it to a study of the effect of nondynamic correlation by doing a more extensive mapping of the PES in a MRCC method. Furthermore, it would be interesting to study the other pathways of ozone depletion along with their inter-reactions. Such developments will be part of a planned systematic study of stratospheric ozone chemistry using a high level theoretical method.

dx.doi.org/10.1021/ct300209s | *J. Chem. Theory Comput.* XXXX, XXX, XXX−XXX

■ ASSOCIATED CONTENT

Supporting Information

Cartesian coordinates of CCSD(T) optimized geometries, vibrational freqency, and infrared intensity. This information is available free of charge via the Internet at http://pubs.acs.org.

■ AUTHOR INFORMATION

Corresponding Author

*E-mail: s.pal@ncl.res.in.

Notes

The authors declare no competing financial interest.

■ ACKNOWLEDGMENTS

The authors acknowledge the facilities of the Center of Excellence in Scientific Computing at NCL. One of the authors, A.K.D., would like to thank the Council of Scientific and Industrial Research (CSIR) for a Senior Research Fellowship. S.P. acknowledges a grant from the DST J. C. Bose Fellowship project and a CSIR SSB Grant towards completion of the work. N.V. would like to thank the Department of Science and Technology, India, for financial support.

■ REFERENCES

(1) Molina, M. J.; Rowland, F. S. *Nature* **1974**, *249*, 810−814.
(2) Crutzen, P. J. *Geophys. Res. Lett.* **1974**, *1*, 205−208.
(3) Rowland, F. S. *Philos. Trans. R. Soc. London, Ser. B* **2006**, *361*, 769−790.
(4) Solomon, S. *Rev. Geophys.* **1999**, *37*, 275−316.
(5) Johnston, H. *Science* **1971**, *173*, 517−522.
(6) Chipperfield, M. P.; Feng, W. *Geophys. Res. Lett.* **2003**, *30*, 1389−1391.
(7) Kinnison, D.; Johnston, H.; Wuebbles, D. *J. Geophys. Res.* **1988**, *93*, 4165−14176.
(8) Randeniya, L. K.; Vohralik, P. F.; Plumb, I. C. *Geophys. Res. Lett.* **2002**, *29*, 1051−1054.
(9) Ravishankara, A. R.; Daniel, J. S.; Portmann, R. W. *Science* **2009**, *326*, 123−125.
(10) Ghormley, J. A.; Ellsworth, R. L.; Hochanadel, C. J. *J. Phys. Chem.* **1973**, *77*, 1341−1345.
(11) Davis, D. D.; Prusazcyk, J.; Dwyer, M.; Kim, P. *J. Phys. Chem.* **1974**, *75*, 1775−1779.
(12) Graham, R. A.; Johnston, H. S. *J. Chem. Phys.* **1974**, *60*, 4628−4629.
(13) Wu, C. H.; Morris, E. D., Jr.; Niki, H. *J. Phys. Chem.* **1973**, *77*, 250−2511.
(14) Bhatia, S. C.; Hall, J. H., Jr. *J. Phys. Chem.* **1980**, *84*, 3255−3259.
(15) Jaroszynska-Wolinska., J. *THEOCHEM* **2010**, *952*, 74−83.
(16) Peiro-Garcia, J.; Nebot-Gil, I. *J. Comput. Chem.* **2003**, *47*, 1657−1663.
(17) (a) Cizek, J. *J. Chem. Phys.* **1966**, *45*, 4256−4266. (b) Bartlett, R. J. *Annu. Rev. Phys. Chem.* **1981**, *32*, 359−402.
(18) Lee, T. J.; Taylor, P. R. *Int. J. Quantum Chem.* **1989**, *S23*, 199−207.
(19) (a) Mukherjee, D. *Pramana* **1979**, *12*, 203−225. (b) Lindgren, I.; Mukherjee, D. *Phys. Rep.* **1987**, *151*, 93−127.
(20) (a) Haque, A.; Kaldor, U. *Chem. Phys. Lett.* **1985**, *117*, 347−351. (b) Haque, A.; Kaldor, U. *Chem. Phys. Lett.* **1985**, *120*, 261−265.
(21) Stanton, J. F.; Bartlett, R. J.; Rittby, C. M. L *J. Chem. Phys.* **1992**, *97*, 5560−5567.
(22) (a) Scheiner, A. C.; Scuseria, G. E.; Rice, J. E.; Lee, T. J.; Schaefer, H. F. *J. Chem. Phys.* **1987**, *87*, 5361−5371. (b) Fitzgerald, G.; Harrison, R. J.; Bartlett, R. J. *J. Chem. Phys.* **1986**, *85*, 5143−5150. (c) Stanton., J. F.; Gauss., J. *J. Chem. Phys.*. **1995**, *103*, 1064−1076.
(23) (a) Salter, E.; Trucks, G.; Bartlett, R. J. *J. Chem. Phys.* **1989**, *90*, 1752−1766. (b) Helgaker, T.; Gauss, J.; Jørgensen, P.; Olsen, J. *J. Chem. Phys.* **1997**, *106*, 6430−6440.
(24) (a) Banerjee, A.; Simons, J. *J. Chem. Phys.* **1982**, *76*, 4548−4559. (b) Laidig, W. D.; Bartlett, R. J. *Chem. Phys. Lett.* **1984**, *104*, 424−430. (c) Mukherjee, D.; Pal, S. *Adv. Quantum Chem.* **1989**, *20*, 291−373.
(25) (a) Evangelista, F. A.; Allena, W. D.; Schaefer, H. F. *J. Chem. Phys.* **2007**, *127*, 024102−024117. (b) Evangelista, F. A.; Simmonett, A. D.; Allen, W. D.; Schaefer, H. F.; Gauss, J. *J. Chem. Phys.* **2008**, *128*, 124104−124116.
(26) (a) Gauss, J; Lauderdale, W. J.; Stanton, J. F.; Watts, J. D.; Bartlett, R. J. *Chem. Phys. Lett.* **1991**, *182*, 207−215. (b) Watts, J. D.; Gauss, J.; Bartlett, R. J. *J. Chem. Phys.* **1993**, *98*, 8718−8733.
(27) (a) Pal, S.; Rittby, M.; Bartlett, R. J.; Sinha, D.; Mukherjee, D. *J. Chem. Phys.* **1988**, *88*, 4357−4366. (b) Pal, S.; Rittby, M.; Bartlett, R. J.; Sinha, D.; Mukherjee, D. *Chem. Phys. Lett.* **1987**, *137*, 273−278. (c) Rittby, M.; Pal, S.; Bartlett, R. J. *J. Chem. Phys.* **1989**, *90*, 3214−3220.
(28) Stanton, J. F.; Bartlett, R. J. *J. Chem. Phys.* **1993**, *98*, 7029−7039.
(29) Melnichuk, A.; Perera, A.; Bartlett, R. J. *Phys. Chem. Chem. Phys.* **2010**, *12*, 9726−9735.
(30) *CFOUR*, coupled-cluster techniques for computational chemistry, a quantum-chemical program package by Stanton, J. F.; Gauss, J.; Harding, M. E.; Szalay, P. G., with contributions from Auer, A. A.; Bartlett, R. J.; Benedikt, U.; Berger, C.; Bernholdt, D. E.; Bomble, Y. J.; Cheng, L.; Christiansen, O.; Heckert, M.; Heun, O.; Huber, C.; Jagau, T.-C.; Jonsson, D.; Juselius, J.; Klein, K.; Lauderdale, W. J.; Matthews, D. A.; Metzroth, T.; ONeill, D. P.; Price, D. R.; Prochnow, E.; Ruud, K.; Schiffmann, F.; Schwalbach, W.; Stopkowicz, S.; Tajti, A.; Vazquez, J.; Wang, F.; Watts, J. D., and the integral packages *MOLECULE* (Almlof, J.; Taylor, P. R.), *PROPS* (Taylor, P. R.), *ABACUS* (Helgaker, T.; Jensen, H. J. Aa.; Jorgensen, P.; Olsen, J.), and *ECP* routines (Mitin, A. V.; van Wullen, C.) For the current version, see http://www.cfour.de.
(31) Frisch, M. J.; Trucks, G. W.; Schlegel, H. B.; Scuseria, G. E.; Robb, M. A.; Cheeseman, J. R.; Scalmani, G.; Barone, V.; Mennucci, B.; Petersson, G. A.; Nakatsuji, H.; Caricato, M.; Li, X.; Hratchian, H. P.; Izmaylov, A. F.; Bloino, J.; Zheng, G.; Sonnenberg, J. L.; Hada, M.; Ehara, M.; Toyota, K.; Fukuda, R.; Hasegawa, J.; Ishida, M.; Nakajima, T.; Honda, Y.; Kitao, O.; Nakai, H.; Vreven, T.; Montgomery, J. A., Jr.; Peralta, J. E.; Ogliaro, F.; Bearpark, M.; Heyd, J. J.; Brothers, E.; Kudin, K. N.; Staroverov, V. N.; Kobayashi, R.; Normand, J.; Raghavachari, K.; Rendell, A.; Burant, J. C.; Iyengar, S. S.; Tomasi, J.; Cossi, M.; Rega, N.; Millam, N. J.; Klene, M.; Knox, J. E.; Cross, J. B.; Bakken, V.; Adamo, C.; Jaramillo, J.; Gomperts, R.; Stratmann, R. E.; Yazyev, O.; Austin, A. J.; Cammi, R.; Pomelli, C.; Ochterski, J. W.; Martin, R. L.; Morokuma, K.; Zakrzewski, V. G.; Voth, G. A.; Salvador, P.; Dannenberg, J. J.; Dapprich, S.; Daniels, A. D.; Farkas, A.; Foresman, J. B.; Ortiz, J. V.; Cioslowski, J.; Fox, D. J. *Gaussian 09*, revision A.1; Gaussian, Inc.: Wallingford, CT, 2009.
(32) Vaval, N.; Ghose, K. B.; Pal, S.; Mukherjee, D. *Chem. Phys. Lett.* **1993**, *209*, 292−298.
(33) Kendall, R. A.; Dunning, T. H.; Harrison, R. J. *J. Chem. Phys.* **1992**, *96*, 6796−6806.
(34) Sander, S. P.; Abbatt, J.; Barker, J. R.; Burkholder, J. B.; Friedl, R. R.; Golden, D. M.; Huie, R. E.; Kolb, C. E.; Kurylo, M. J.; Moortgat, G. K.; Orkin, V. L.; Wine, P. H. *Chemical Kinetics and Photochemical Data for Use in Atmospheric Studies*, Evaluation No. 17, JPL Publication 10−6, Jet Propulsion Laboratory: Pasadena, CA, 2011. http://jpldataeval.jpl.nasa.gov (accessed Mar. 2012).
(35) Thompson, B. A.; Harteck, P; Reeves, R. R. *J. Geophys. Res.* **1963**, *68*, 6431−6436.
(36) (a) Barbe, A.; Secroun, C.; Jouve, P. *J. Mol. Spectrosc.* **1974**, *49*, 171−182. (b) Tanaka, T.; Morino, Y. *J. Mol. Spectrosc.* **1970**, *33*, 538−551.
(37) Huber, H. P.; Herzberg, G. *Molecular Structure and Molecular Spectra IV.Constants of Diatomic Molecules*; Van Nostrand Reinhold: Toronto, 1979.
(38) Ruden, T. A.; Helgaker, T.; Jørgensen, P.; Olsen., J *J. Chem. Phys.* **2004**, *121*, 5874−5884.

(39) (a) Wilkinson, I.; Whitaker, B. J. *J. Chem. Phys.* **2008**, *129*, 154312−154326. (b) Schinke, R; Suarez, J; Farantos, S. C. *J. Chem. Phys.* **2010**, *133*, 091103−091106.
(40) Logan, J. A. *J. Geophys. Res.* **1983**, *88*, 10785−10807.
(41) Crutzen, P. J. *Ann. Rev. Earth Planet. Sci.* **1979**, *7*, 443−472.
(42) Logan, J. A.; Prather, M. J.; Wofsy, S. C.; McElroy, M. B. *EOS Trans. Am. Geophys. Union* **1978**, *59*, 36−42.
(43) Demore, W. B.; Sander, S. P.; Golden, D. M.; Hampson, R. F.; Kurylo, M. J.; Howard, C. J.; Ravishankara, A. R.; Kolb, C. E.; Molina, M. J. *Chemical Kinetics and Photochemical Data for Use in Atmospheric Studies*, Evaluation No. 11, JPL Publication 94−26, Jet Propulsion Laboratory: Pasadena, CA, 1994. http://jpldataeval.jpl.nasa.gov (accessed Mar 2012).
(44) Dupuis, M.; Fitzgerald, G.; Hammond, B.; Lester, W. A.; Schaefer, H. F. *J. Chem. Phys.* **1986**, *84*, 2691−2697.
(45) (a) Clyne, M. A. A.; Thrush, B. A.; Wayne, R. P. *Trans. Faraday Soc.* **1964**, *60*, 359−370. (b) Stedman, D. H.; Niki, H. *J. Phys. Chem.* **1973**, *77*, 2604−2609. (c) Lippmann, H. H.; Jesser, B.; Schurath, U. *Int. J. Chem. Kinet.* **1980**, *12*, 547−554. (d) Borders, R. A.; Birks, J. W. *J. Phys. Chem.* **1982**, *86*, 3295−3302.
(46) Davis, H. F.; Kim, B. S.; Johnston, H. S.; Lee, Y. T. *J. Phys. Chem.* **1993**, *97*, 2172−2180.
(47) Eisfield, W.; Morokuma, K. *J. Chem. Phys.* **2003**, *119*, 4682−4688.
(48) Olson, L. P.; Kuwata, K. T.; Bartberger, M. D.; Houk, K. N. *J. Am. Chem. Soc.* **2002**, *124*, 9469−9475.
(49) Morris, V. R.; Bhatia, S. C.; Hall, J. H. *J. Phys. Chem.* **1990**, *94*, 7414−7418.